Electronic Supplementary Information

A series of Benzothiazole based Schiff bases for colorimetric sensing of fluoride and acetate ions: acetate induced "turn-on" fluorescence for selectivity

Nilotpal Borah, Sagnik De, Abhijit Gogoi, Gopal Das*

Department of Chemistry, Indian Institute of Technology Guwahati, Assam-781039, India Fax: +91-361-2582349; Tel: +91-361-2582313;

E-mail: gdas@iitg.ac.in

The chemosensors $\mathbf{L_1}$ and $\mathbf{L_3}$ were synthesized and reported from our group earlier and hence similar synthetic and characterization procedure were followed. In case of $\mathbf{L_1}$, the solvent for ^{1}H NMR has been altered from $CDCl_3$ in earlier case to DMSO-d_6 for better solubility.

$\mathbf{L_1}$, ^{1}H NMR (600 MHz, DMSO-d_6, $SiMe_4$) δ(ppm): 12.19 (bs, 1H, hydrazone –NH), 9.19 (s, 1H, imine –CH), 8.66-8.65 (d, 1H, Ar_H), 7.91-7.87 (t, 2H, Ar_H), 7.72-7.75 (m, 1H, Ar_H), 7.60-7.57 (t, 1H, Ar_H), 7.42-7.39 (t, 1H, Ar_H), 7.32-7.29 (t, 2H, Ar_H), 7.25-7.24 (d, 1H, Ar_H), 7.12-7.10 (t, 1H, Ar_H).

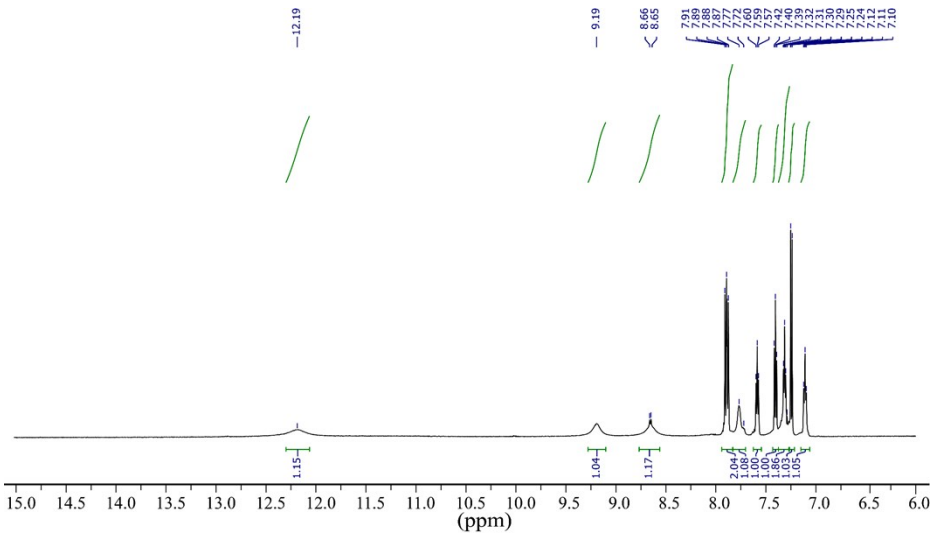

Figure S1. ^{1}H NMR of $\mathbf{L_1}$ in DMSO at 298 K.-

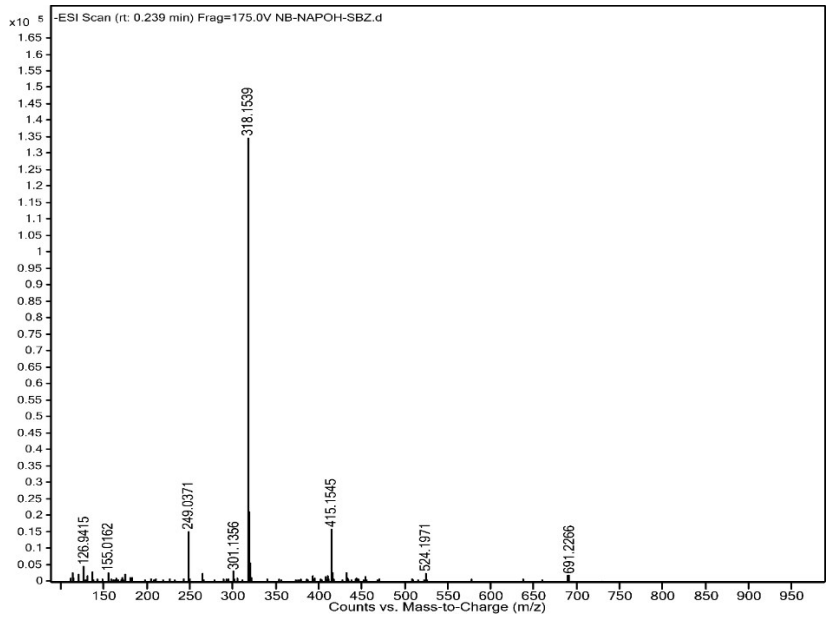

Figure S2. ESI-Mass spectrum of receptor $\mathbf{L_1}$ in acetonitrile (negative mode).

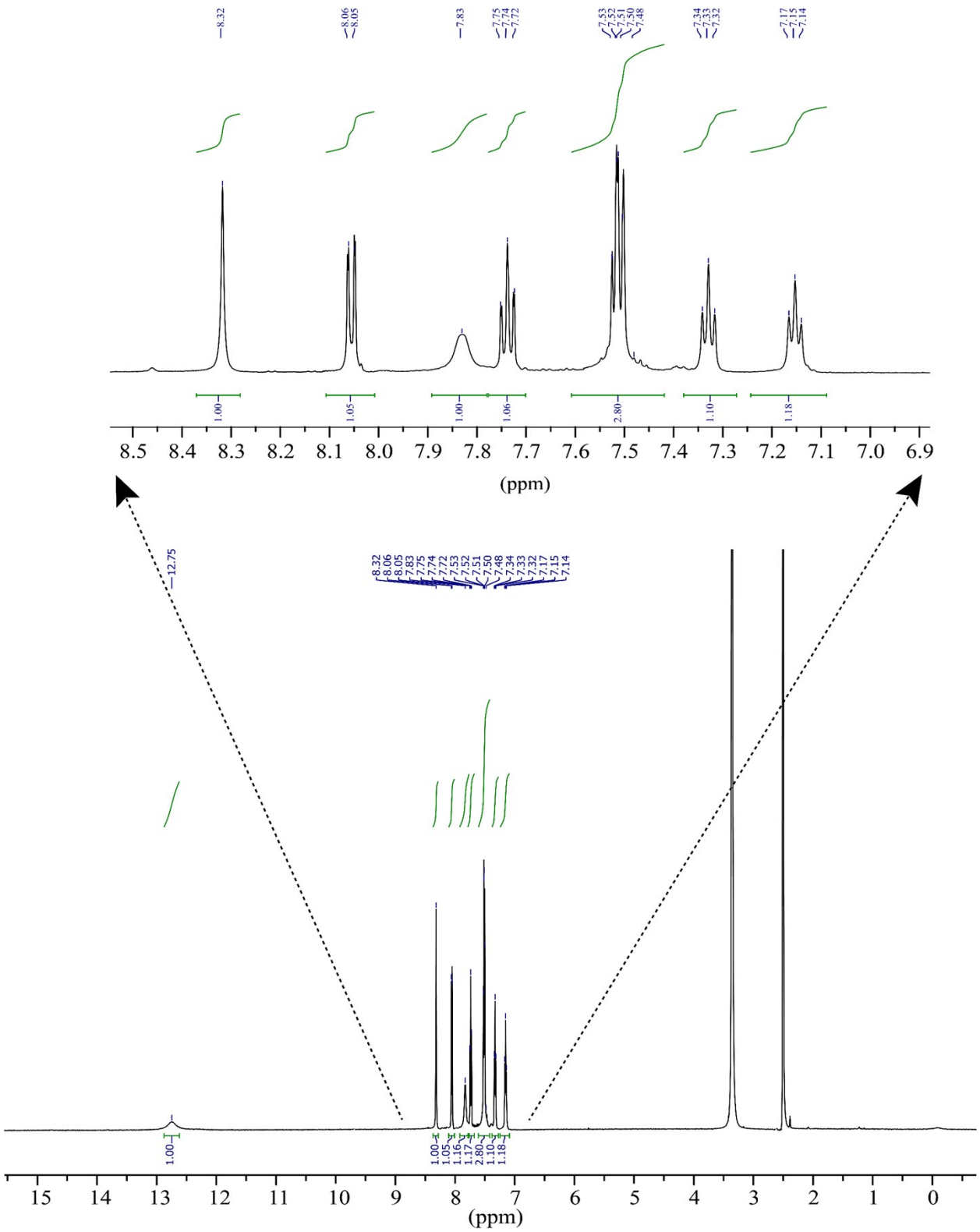

Figure S3. Expanded ^{1}H NMR of **L_2** in DMSO-d_6 at room temperature.

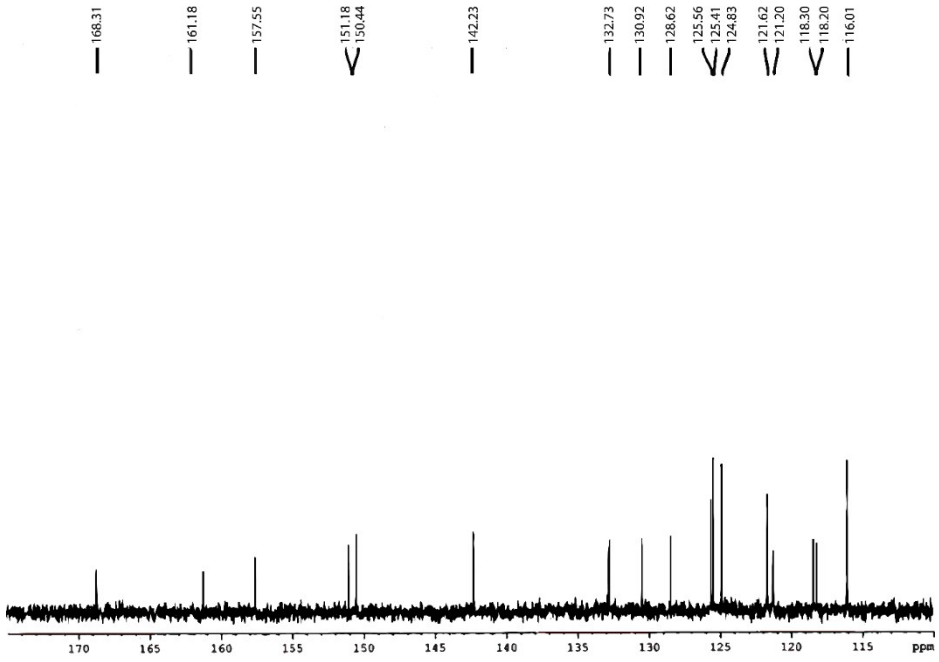

Figure S4. ^{13}C NMR of $\mathbf{L_2}$ in DMSO-d_6

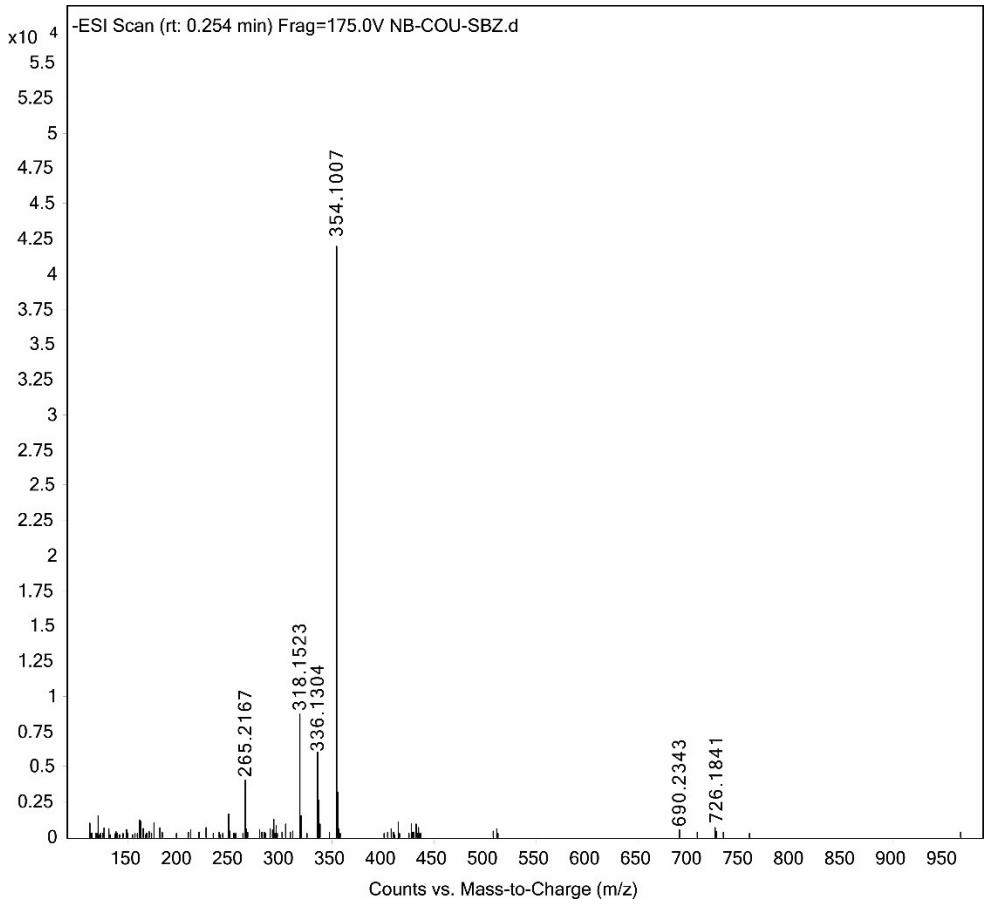

Figure S5. ESI-Mass spectrum of receptor $\mathbf{L_2}$ in acetonitrile (negative mode).

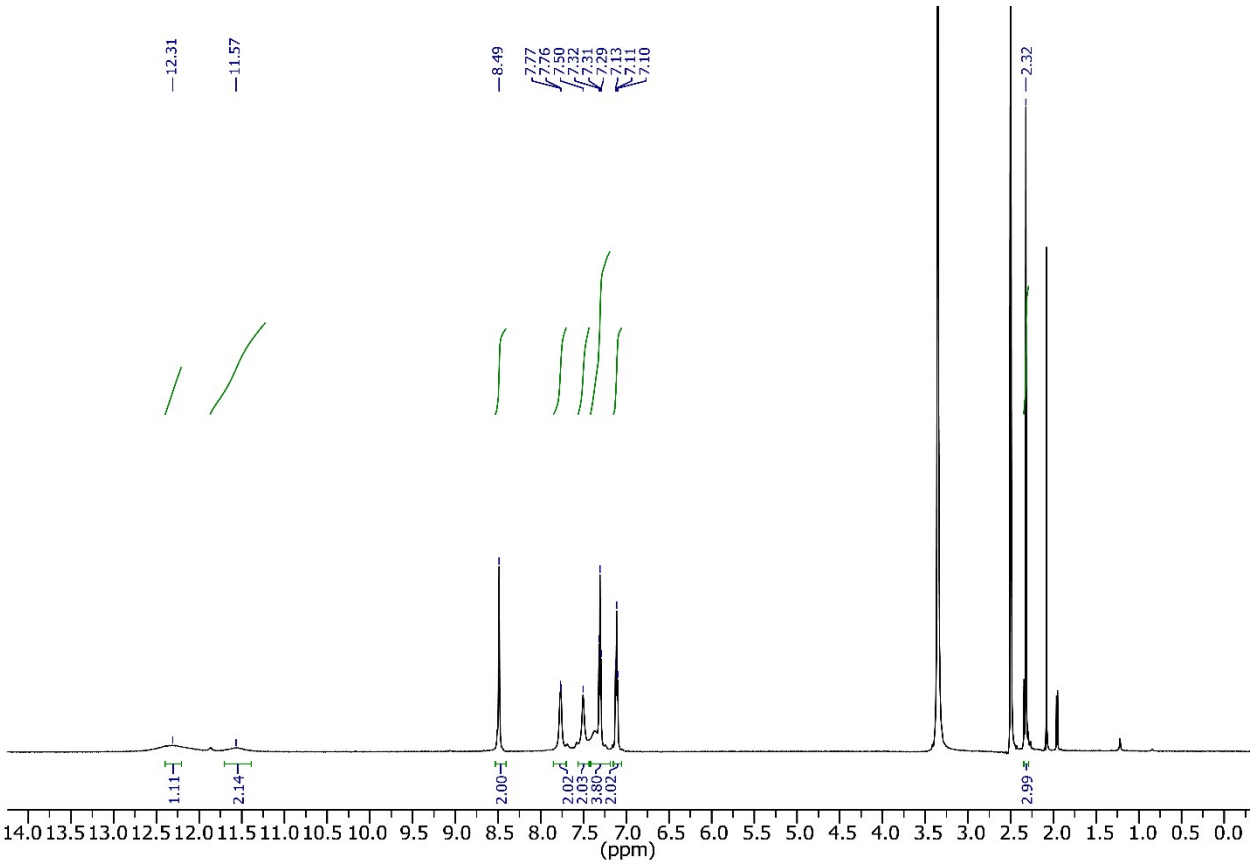

Figure S6. ^{1}H NMR of $\mathbf{L_3}$ in DMSO at 298 K.

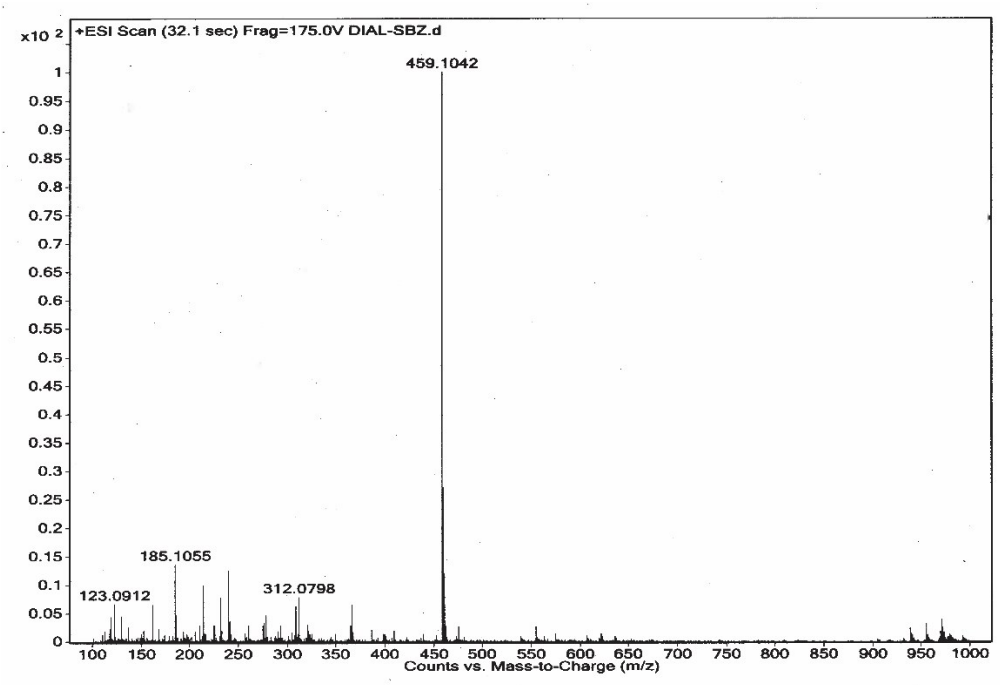

Figure S7. ESI-Mass spectrum of receptor $\mathbf{L_3}$ in acetonitrile (positive mode).

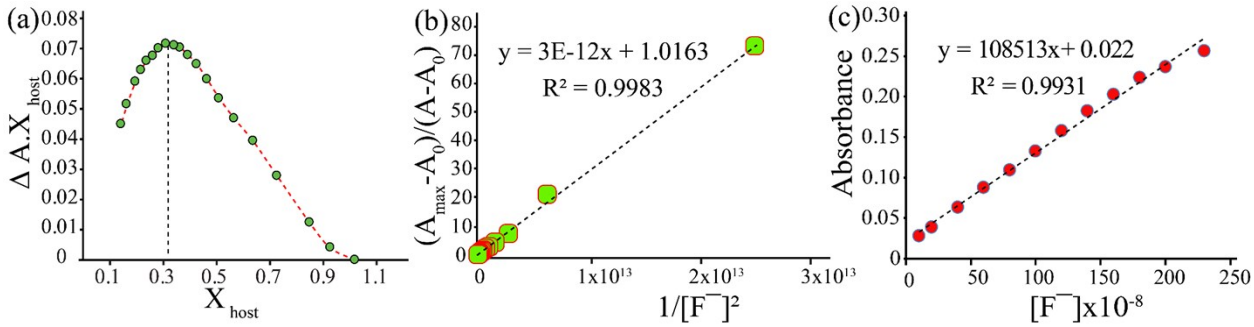

Figure S8. a) Job's plot for determining the stoichiometry of the probe $\mathbf{L_1}$ and F^- ion and (b) The corresponding Benesi−Hildebrand plot for binding constant determination. (c) Absorbance intensity at 456 nm versus F^- ion concentrations for lowest detection limits (LOD) calculation.

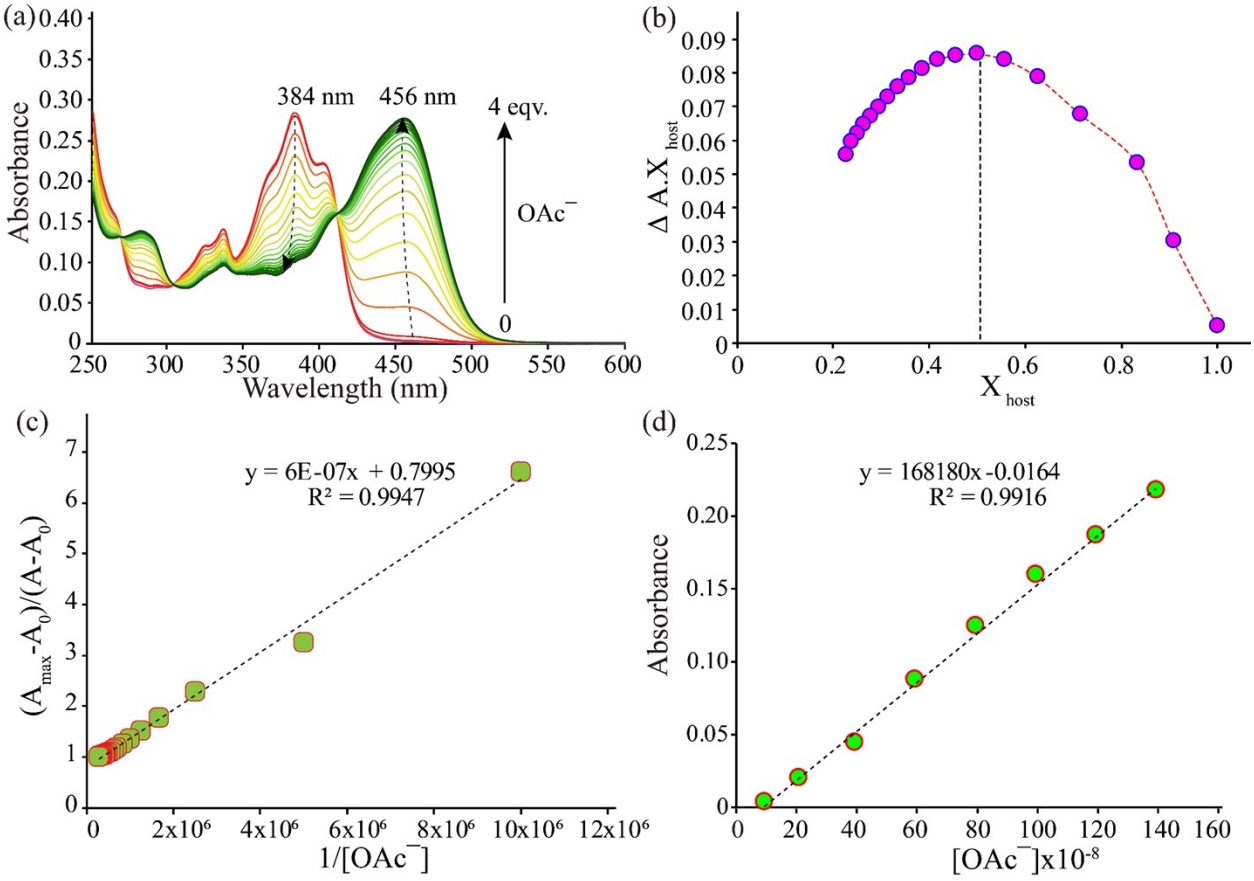

Figure S9. (a) UV–vis titration spectra of the probe $\mathbf{L_1}$ upon incremental addition of OAc^- ion (0–4 eqv.) in CH_3CN. (b) Job's plot for determining the stoichiometry of the probe $\mathbf{L_1}$ and OAc^- ion and (c) The corresponding Benesi−Hildebrand plot for binding constant determination. (d) Absorbance intensity at 456 nm versus OAc^- ion concentrations for lowest detection limits (LOD) calculation.

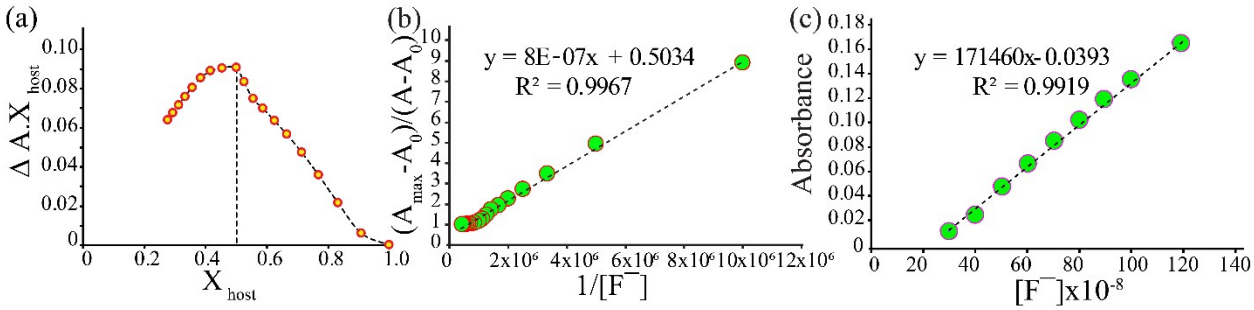

Figure S10. a) Job's plot for determining the stoichiometry of the probe **L_2** and F^- ion and (b) The corresponding Benesi−Hildebrand plot for binding constant determination. (c) Absorbance intensity at 550 nm versus F^- ion concentrations for lowest detection limits (LOD) calculation.

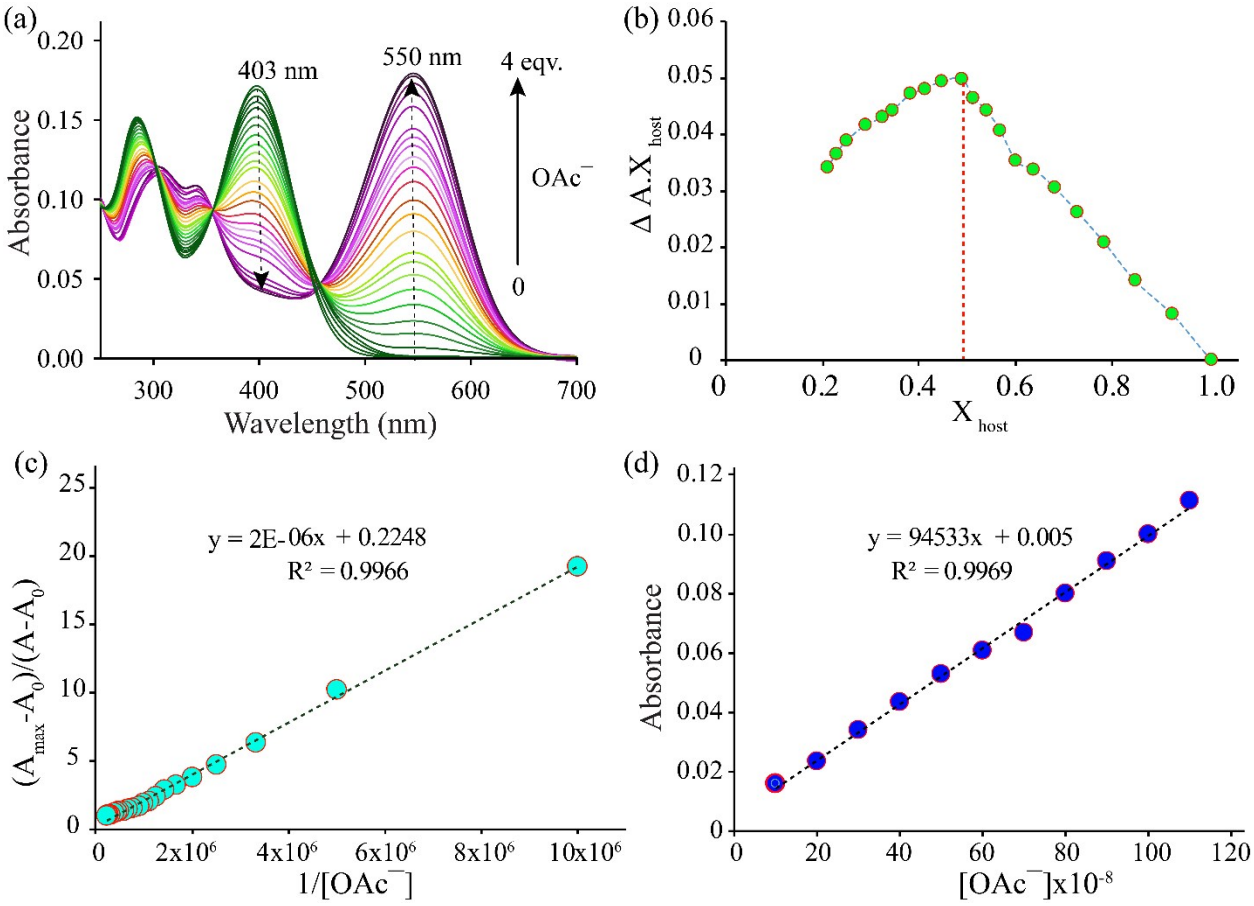

Figure S11. (a) UV–vis titration spectra of the probe **L_2** upon incremental addition of OAc^- ion (0–4 eqv.) in CH_3CN. (b) Job's plot for determining the stoichiometry of the probe **L_2** and OAc^- ion and (c) The corresponding Benesi−Hildebrand plot for binding constant determination. (d) Absorbance intensity at 550 nm versus OAc^- ion concentrations for lowest detection limits (LOD) calculation.

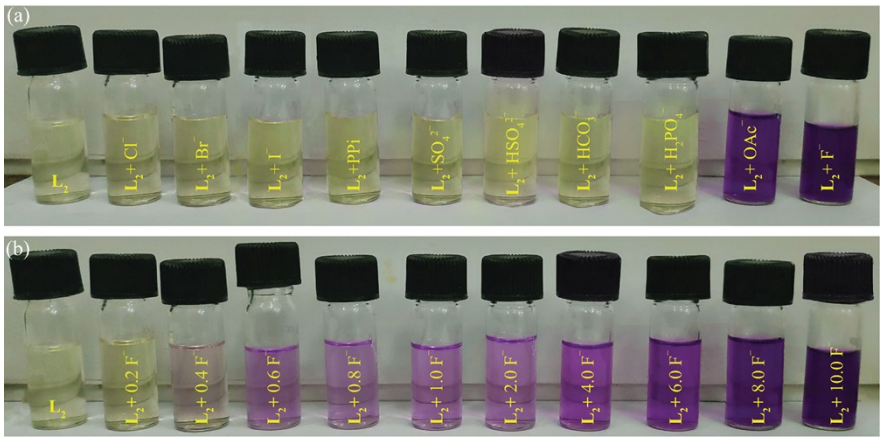

Figure S12. (a) Naked eye sensing of F^- and OAc^- using probe $\mathbf{L_2}$ in acetonitrile (b) Colorimetric change of $\mathbf{L_2}$ solution with addition of fluoride ion till 10 eqvt.

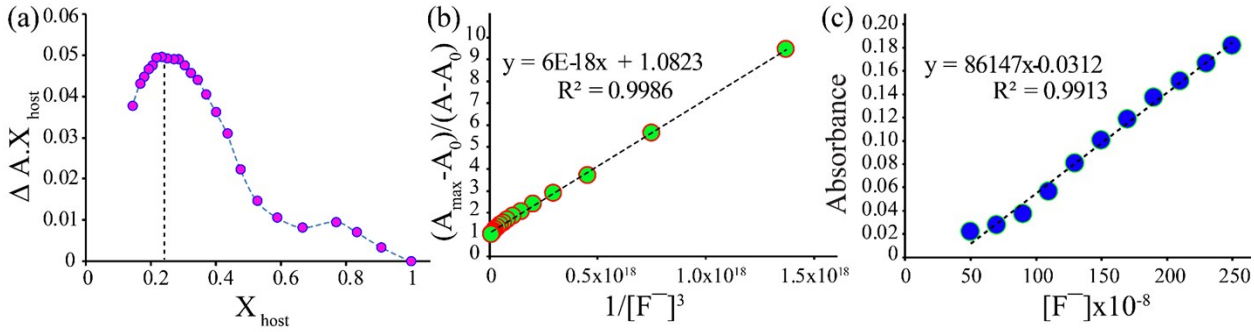

Figure S13. (a) Job's plot for determining the stoichiometry of the probe $\mathbf{L_3}$ and F^- ion and (b) The corresponding Benesi−Hildebrand plot for binding constant determination. (c) Absorbance intensity at 450 nm versus F^- ion concentrations for lowest detection limits (LOD) calculation.

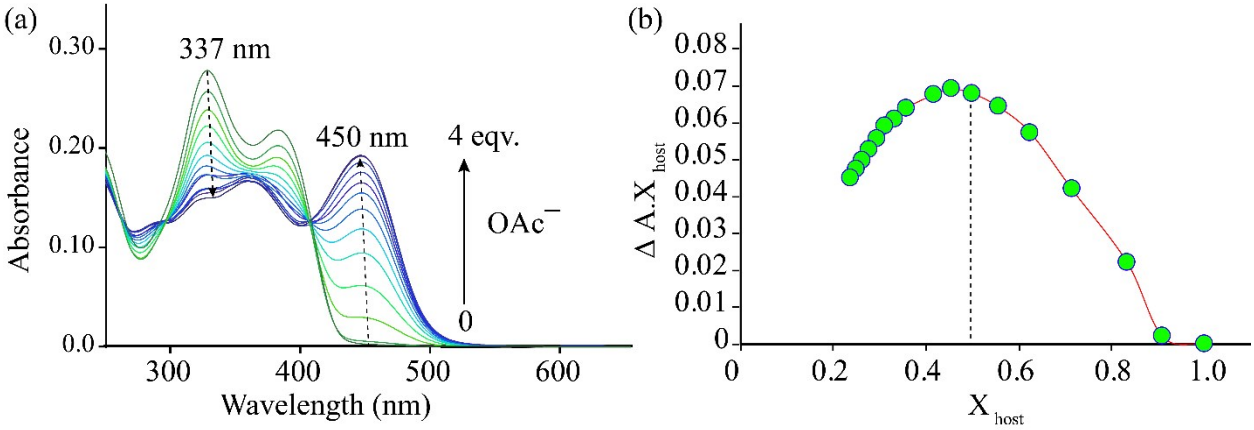

Figure S14. (a) UV-Vis absorption change of $\mathbf{L_3}$ with increasing concentration of OAc^-. (b) The corresponding Job's plot and (c) Benesi−Hildebrand plot for binding constant determination.

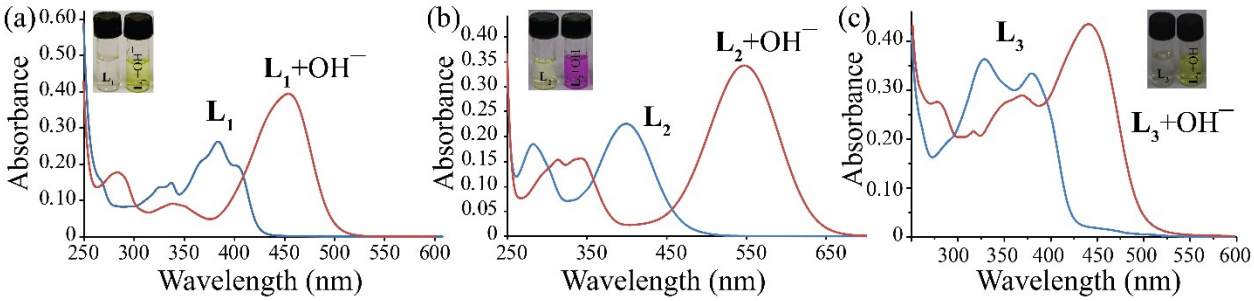

Figure S15. Comparative absorption spectra of hydroxide addition to the chemosenors (a) $\mathbf{L_1}$, (b) $\mathbf{L_2}$, and (c) $\mathbf{L_3}$ in acetonitrile. Inset: Visible colour change upon addition of the hydroxide anions to the probe solutions.

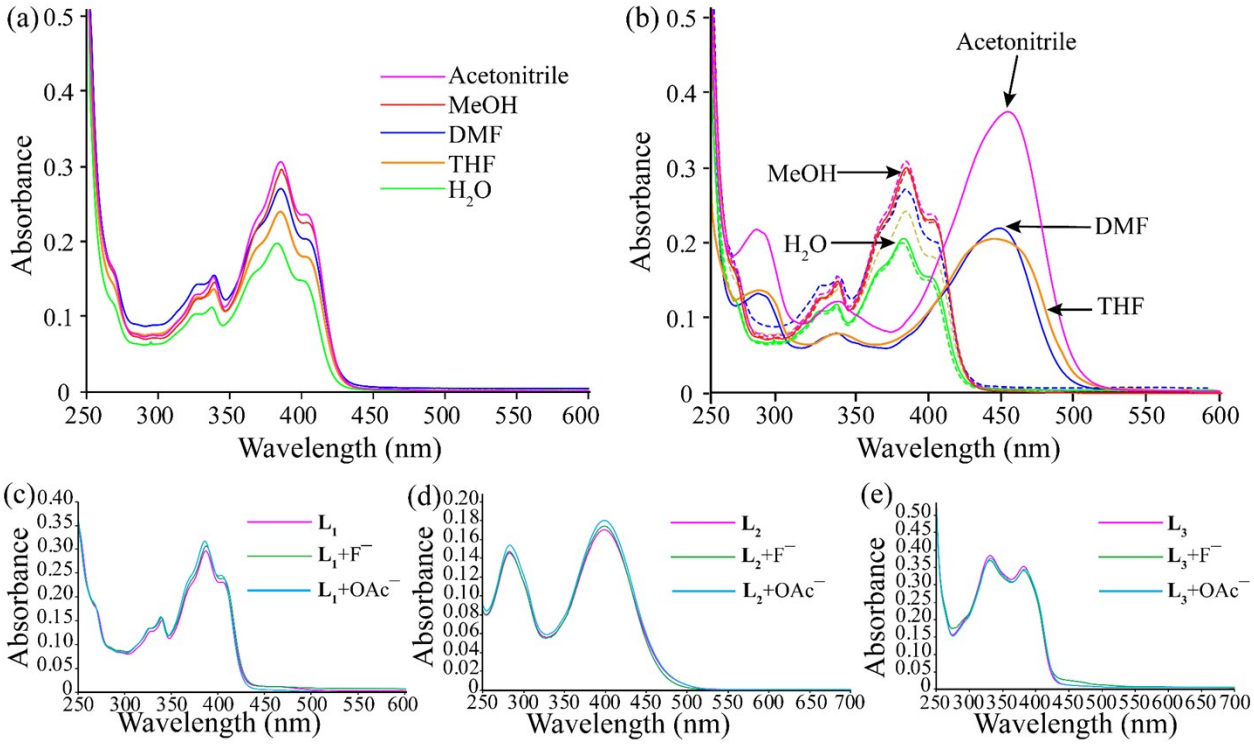

Figure S16. (a) Absorption spectra of $\mathbf{L_1}$ (10 mM) in different solvents. (b) Corresponding change in the absorption specta of $\mathbf{L_1}$ in different solvent in presence of fluoride anion (50 mM) (Dotted line represents the original absorption spectra in absence of the anion). (c) Change in absorption spectra of $\mathbf{L_1}$ in acetonitrile: H_2O=4:1solution (10 mM) with fluoride and acetate anion (50 mM). (d) Change in absorption spectra of $\mathbf{L_2}$ in acetonitrile: H_2O=4:1solution (10 mM) with fluoride and acetate anion (50 mM). (e) Change in absorption spectra of $\mathbf{L_3}$ in acetonitrile: H_2O=4:1solution (10 mM) with fluoride and acetate anion (50 mM).

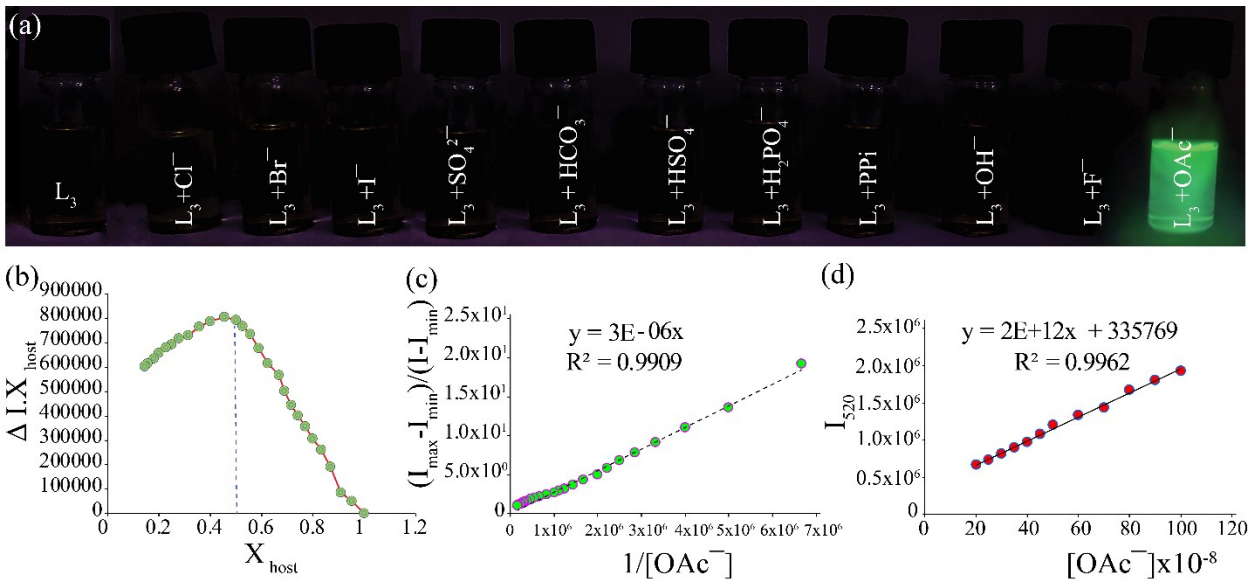

Figure S17. (a)Visual changes in fluorescence of $\mathbf{L_3}$ under UV light (λ_{ex} = 365 nm) in Acetonitrile. (b) Job's plot for determining the stoichiometry of the probe $\mathbf{L_3}$ and OAc^- ion and (c) The corresponding Benesi−Hildebrand plot for binding constant determination. (d) Fluorescence intensity at 520 nm versus OAc^- ion concentrations for lowest detection limits (LOD) calculation.

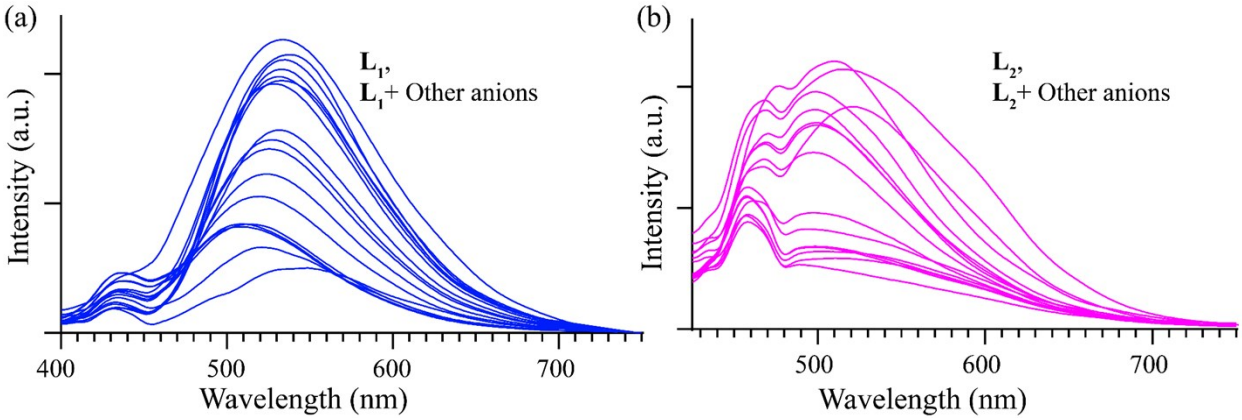

Figure S18. Fluorescence emission changes of (a) $\mathbf{L_1}$ and (b) $\mathbf{L_2}$ with various anions.

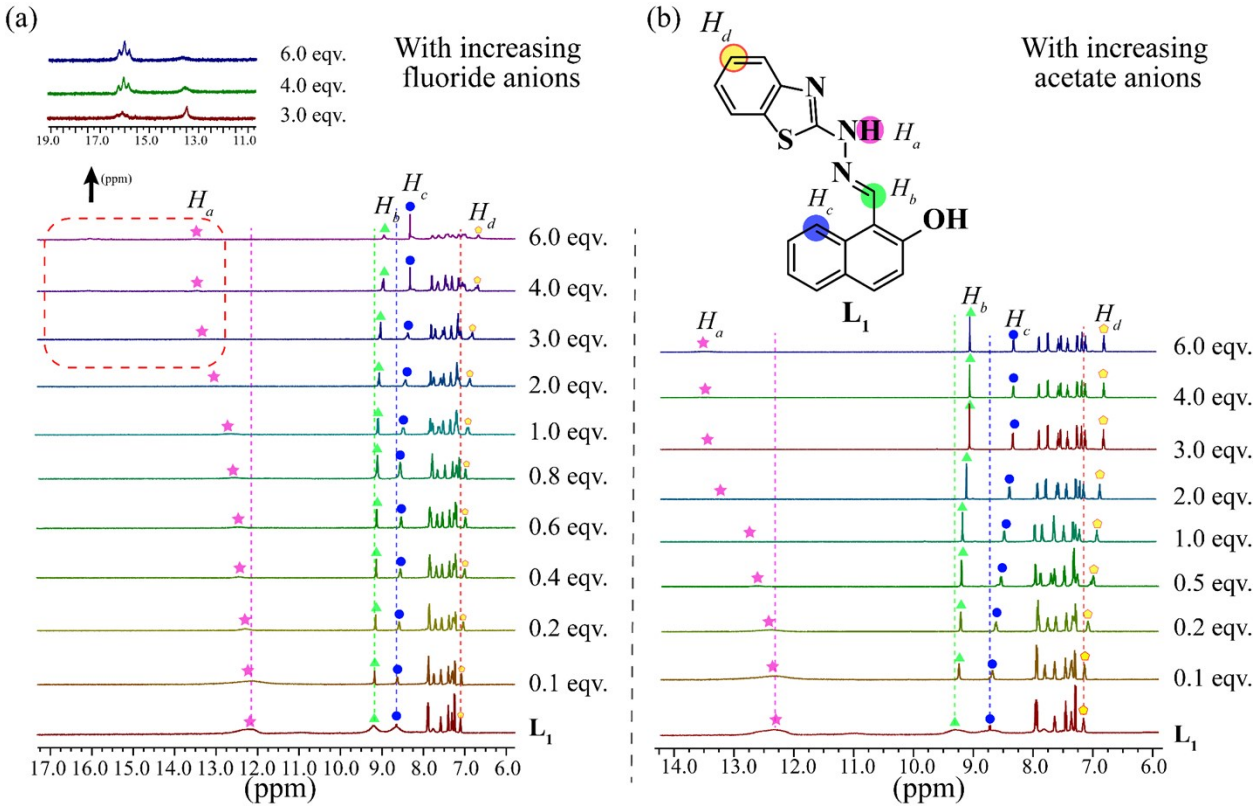

Figure S19. Stack plot of the ^{1}H NMR spectra of receptor $\mathbf{L_1}$ in the presence of increasing amounts of (a) TBAF (0.1-6.0 equiv.) and (b) TBAOAc (0.1-6.0 equiv.) recorded in DMSO-d_6.

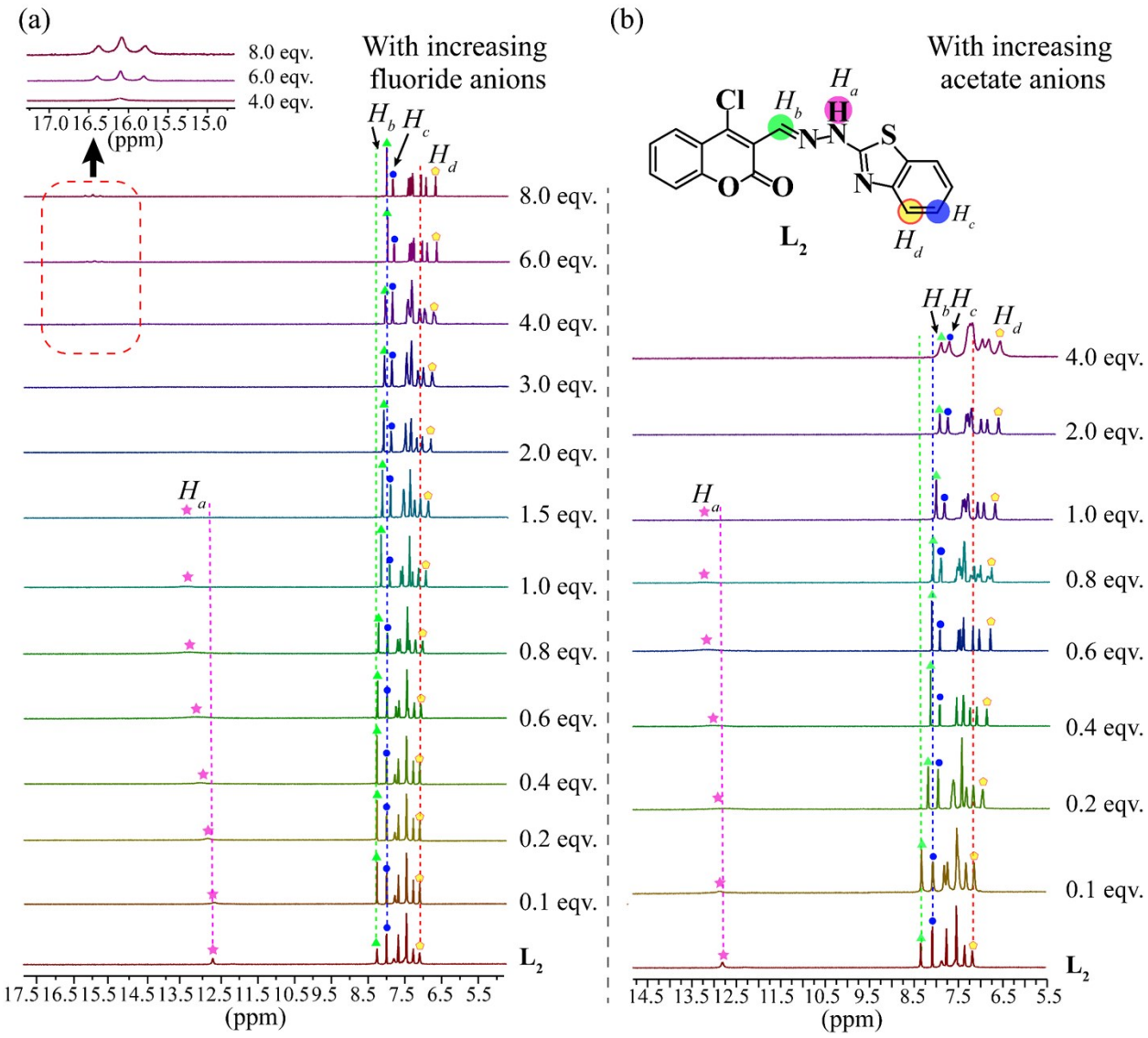

Figure S20. Stack plot of the ^{1}H NMR spectra of receptor $\mathbf{L_2}$ in the presence of increasing amounts of (a) TBAF (0.1-8.0 equiv.) and (b) TBAOAc (0.1-4.0 equiv.) recorded in DMSO-d_6.

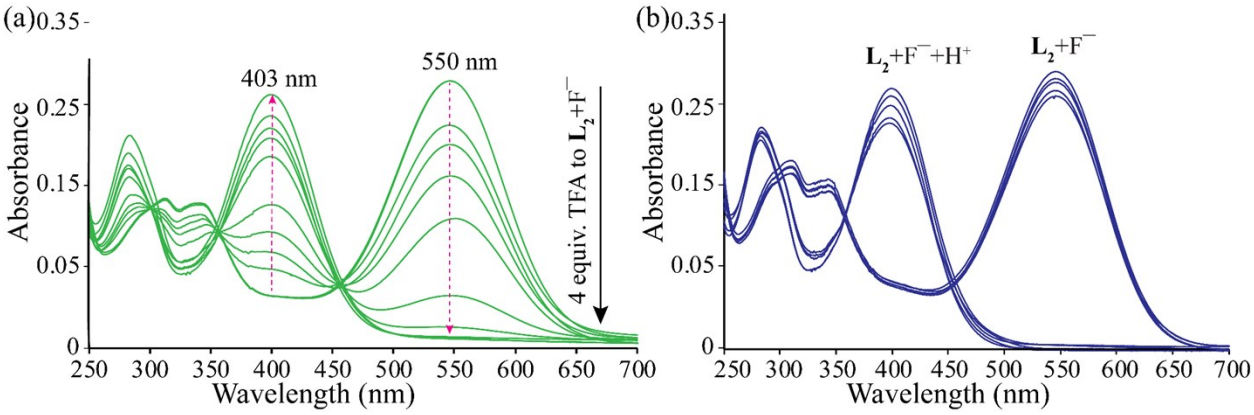

Figure S21. (a) Titration of $\mathbf{L_2}$- F^- complex with Trifluoroacetic acid. (b) Reversibility test of the probe $\mathbf{L_2}$; Bathochromatic shift of 147 nm with the addition of fluoride ions (F^-) and reversed back to the original upon addition of TFA (upto 5 cycles).

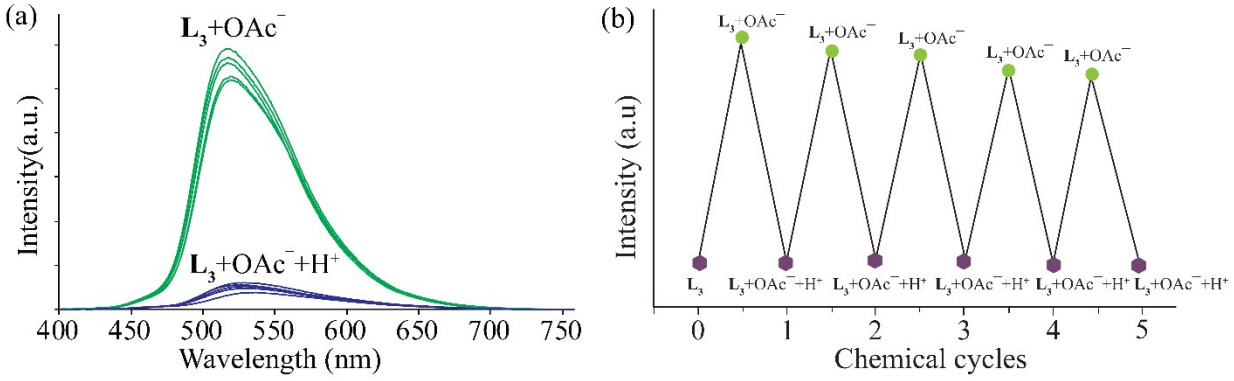

(c)

Inp1 ($\mathbf{L_2}$)	Inp2 (OAc^-)	Inp3 (H^+)	Out $_{(520)}$
0	0	0	0
0	0	1	0
0	1	0	0
0	1	1	0
1	0	0	0
1	0	1	0
1	1	0	1
1	1	1	0

(d)

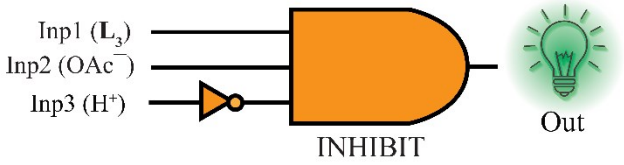

Figure S22. (a) Reversible and recyclable behaviour of probe $\mathbf{L_3}$ on addition of TBAOAc and TFA. (b) Reversibility of UV-Vis response of $\mathbf{L_3}$ (up to five cycles) with alternate addition of OAc^- and H^+. (c) and (d) The truth table for the fabricated 'INHIBIT' logic gate based on the probe behaviour towards OAc^- and H^+.

Table S1. The comparison of our chemosensors with Schiff base based F^- and/or acetate sensors available in recent literatures.

Sl No.	References	LOD for fluoride	LOD for acetate	Solvent system	Remarks
1	Our chemosensors	3.35×10^{-8} M by $\mathbf{L_2}$	2.907×10^{-8} M by $\mathbf{L_3}$	Acetonitrile	$\mathbf{L_2}$ Colorimetric fluoride sensor, $\mathbf{L_3}$ Turn on Fluorescent Acetate sensor
2	G. G. G. Kumar, M. P. Kesavan, G. Sivaraman, J. Rajesh, *Sensors and Actuators B*, 2018, **255**, 3194-3206.	0.30 μM	NA	PBS buffer	Colorimetric and NIR fluoride sensor
3	D. Sharma, A. Kuba, R. Thomas, S. K. A. Kumar, A. Kuwar, H. -J. Choi, and S. K. Sahoo, *Spectrochimica Acta Part A: Molecular and Biomolecular Spectroscopy,* 2016, **157**, 110–115.	NA	7.37×10^{-6} M	DMSO: H_2O (95:5)	Acetate selective fluorescent turn-on sensor
4	Q. Lin, X. Liu, T.-B. Wei, Y.-M. Zhang, *Sensors and Actuators B*, 2014, **190**, 459– 463.	NA	4.0×10^{-7} M	DMSO	Acetate selective fluorescent turn-on sensor
5	C.-B. Bai, J. Zhang, R. Qiao, S.-Y. Mu, M. Meng, B. Wei, C. Wang, C.-Q. Qu, and Y.-T. Ji, *SN Applied Sciences*, 2020, **2**, 567.	NA	4.6×10^{-9} M	HEPES Buffer: acetonitrile (2:8)	Acetate selective fluorescent turn-on sensor
6	G. R. Youa, G. Ji. Park, S. A. Lee, Y. W. Choi, Y. S. Kim, J. J. Lee, and C. Kim, *Sensors and Actuators B*, 2014, **202** 645–655.	NA	140.0×10^{-6} M	DMSO/bis–tris buffer (8:2)	Colorimetric acetate sensor
7	S. Goswami, S. Maity, A. C. Maity, A. K. Das, B. Pakhira, K. Khanra, N. Bhattacharyya, and S. Sarkar, *RSC Adv.*, 2015, **5**, 5735-5740.	12.7 μM	NA	Acetonitrile	Fluoride selective fluorescent turn-on sensor
8	S. Ghosha, A. Gangulya, A. Bhattacharyya, M. A. Alam, and N. Guchhait, *RSC Adv.*, 2016, **6**, 67693-67700.	1.3μM	NA	Acetonitrile	Colorimetric fluoride sensor